(10) Swislow, G.; Sun, S. T.; Nishio, I.; Tanaka, T. *Phys. Rev. Lett.* **1980**, *44*, 796.
(11) Sun, S. T.; Nishio, I.; Swislow, G.; Tanaka, T. *J. Chem. Phys.* **1980**, *73*, 5971.
(12) Miyaki, Y.; Fujita, H. *Polym. J.* **1981**, *13*, 749.
(13) Oyama, T.; Shiokawa, K.; Baba, K. *Polym. J.* **1981**, *13*, 167.
(14) Stapanek, P.; Konak, C.; Sedlacek, B. *Macromolecules* **1982**, *15*, 2141.
(15) Perzynski, R.; Adam, M.; Delsanti, M. *J. Phys. (Les Ulis, Fr.)* **1982**, *43*, 129.
(16) Perzynski, R.; Delsanti, M.; Adam, M. *J. Phys. (Les Ulis, Fr.)* **1984**, *45*, 1765.
(17) Vidakovic, P.; Rondelez, F. *Macromolecules* **1984**, *17*, 418.
(18) Selser, J. C. *Macromolecules* **1985**, *18*, 585.
(19) Park, I. H.; Wang, Q.-W.; Chu, B. *Macromolecules* **1987**, *20*, 1965.
(20) Saeki, S.; Konno, S.; Kuwahara, N.; Nakata, M.; Kaneko, M. *Macromolecules* **1974**, *7*, 521.
(21) Kubota, K.; Abbey, K. M.; Chu, B. *Macromolecules* **1983**, *16*, 137.
(22) De Gennes, P.-G. *J. Phys. Lett.* **1975**, *36*, L55.
(23) Sanchez, I. C. *Macromolecules* **1979**, *12*, 980.
(24) Akcasu, A. Z.; Han, C. C. *Macromolecules* **1979**, *12*, 276.
(25) Farnoux, B.; et al. *J. Phys. (Les Ulis, Fr.)* **1978**, *39*, 77.
(26) Huglin, M. B., Ed. *Light Scattering from Polymer Solutions*; Academic: New York, 1972.
(27) Chu, B. *Laser Light Scattering*; Academic: New York, 1974.
(28) Berne, B. J., Pecora, P., Eds. *Dynamic Light Scattering*; Wiley: New York, 1976.
(29) Stockmayer, W. H.; Schmidt, M. *Pure Appl. Chem.* **1982**, *54*, 407.
(30) Schmidt, M.; Burchard, W. *Macromolecules* **1981**, *14*, 210.
(31) Washburn, E. W., Ed. *International Critical Tables of Numerical Data, Physics, Chemistry and Technology*; McGraw-Hill: New York, 1926.

Influence of Solvent Casting on the Evolution of Phase Morphology of PC/PMMA Blends

Jeanne M. Saldanha and Thein Kyu*

Center for Polymer Engineering, The University of Akron, Akron, Ohio 44325.
Received February 20, 1987

ABSTRACT: The effect of solvent casting on the structure evolution of bisphenol A polycarbonate (PC) and polymethyl methacrylate (PMMA) mixtures has been investigated as a function of solvent evaporation rate, casting temperatures, and the kind of solvent used. The casting conditions exert profound effects on the final blend morphology. PC/PMMA blends cast from tetrahydrofuran (THF) at low temperatures (20 °C or below) exhibit phase separation behavior as well as solvent-induced crystallization in the PC phase. The solvent casting at ambient (23 °C) shows the development of a modulated biphase structure with high level of interconnectivity characteristic of spinodal decomposition. However, the casting at an elevated temperature (47 °C) yields transparent amorphous films with a single glass transition (T_g) located at intermediate temperatures between those of pure polymers and varies systematically with composition. Cloud-point measurements on the PC/PMMA system reveal a miscibility window reminiscent of an LCST (lower critical solution temperature). Solvent casting of PC/PMMA blends from cyclohexanone (CHN) generally results in phase separation accompanied by crystallization of the PC phase. The casting from methylene chloride (MC) shows no indication of solvent-induced crystallization, but the system phase separates during solvent evaporation. The mechanisms of phase separation and crystallization during solvent evaporation have been investigated by means of time-resolved light scattering, and the results are analyzed in the context of a pseudobinary approximation.

I. Introduction

Thermodynamic and kinetic studies of polymer phase separation[1-9] have made considerable progress. However, the general perception is that most polymer pairs are immiscible as a result of low entropy of mixing associated with long molecular structures of polymers. This notion has changed gradually since polymer miscibility can be enhanced through some specific interactions between dissimilar molecules. Additional factors such as blending conditions were found to play an important role in miscibility studies.[10] A number of mixing techniques have been employed in the preparation of polymer blends, among which mechanical mixing and solvent blending are common methods widely practiced in industries and many laboratories. It is, however, difficult to obtain homogeneous polymer mixtures with the former method. The latter method generally gives a better mix. Even in solvent blending, several techniques, namely, solution casting, freeze drying, or coprecipitation have been adopted as can be witnessed in the literature.[1-12] Little attention has been paid to the detailed procedure; however, this turns out to be very important according to the recent studies.[10,11,13]

Varnell and co-workers[10] demonstrated the effect of solvent casting on crystallization and miscibility of polycarbonate (PC)/polycaprolactone (PCL) blends. They found that when PC/PCL were cast from tetrahydrofuran (THF), PC phase resulted in crystallization, whereas the casting from methylene chloride (MC) showed no sign of crystallization in PC phase. This behavior has been attributed to differences in the rate of solvent evaporation and the interaction between solvents and polymers. The authors concluded that the strong interaction (the hydrogen bonding) was responsible for miscibility enhancement in PC/PCL blends.

The development of modulated structure during solvent casting of polymer blends was reported recently by Inoue et al.[11] on many polymer blend systems, typically poly(methyl methacrylate)/poly(acrylonitrile-*co*-styrene) and poly(vinyl methyl ether)/polystyrene having a lower critical solution temperature (LCST) and poly(methylphenylsiloxane)/polystyrene having an upper critical solution temperature (UCST). They reached a conclusion that the modulated structure resulted from the spinodal decomposition during solvent casting of the ternary blend solution. The thermodynamic aspects of spinodal decomposition have been interpreted in accordance with the procedure of Zeeman and Patterson.[12]

The kinetics of phase separation and phase dissolution of ternary blend solutions were also reported by Hashimoto et al.[13] on polystyrene/styrene-butadiene diblock poly-

0024-9297/87/2220-2840$01.50/0

mers/toluene. During solvent casting, the spatial fluctuations were found to develop and grow in accordance with spinodal decomposition (SD) and its subsequent coalescence mechanisms. The authors demonstrated that the early stage of phase separation in their ternary blend solutions can be characterized by the linearized Cahn–Hilliard theory based on the pseudobinary approximation.

In this paper, the effect of solvent casting on the evolution of phase morphology of polycarbonate (PC)/PMMA blends are explored as a function of casting temperature, the rates, and the kind of solvents used. Time-dependent behavior of solvent-induced phase separation and solvent-induced crystallization processes are investigated for PC/PMMA/THF and PC/PMMA/MC systems. The analysis is undertaken in the context of a pseudobinary approximation, taking into consideration, for instance, PC/THF as one component and PMMA/THF as the other.

II. Experimental Section

A. Materials. Commercial grades of bisphenol A polycarbonate (PC) (Lexan 141, $M_w \simeq 58000$ and $M_w/M_n \simeq 2.7$; GE) and polymethyl methacrylate (PMMA) (V920, $M_w = 85000$, $M_w/M_n = 2.05$, and $T_g = 105$ °C, and V811, $M_w \simeq 84{,}000$, $M_w/M_n \simeq 2.13$, and $T_g = 115$ °C; Rohm & Haas Co.) were used in this study. The molecular weights (M_w) were obtained by light scattering (Sophica), and M_w/M_n were determined by GPC (gel permeation chromatography, Model 150 Waters, with polystyrene standards). V920 is a high-temperature resistant PMMA and has a lower T_g than that of the standard V811.

Various PC/PMMA blend solutions were prepared by dissolving in THF, MC, and cyclohexanone (CHN). The polymer concentration was 2% by weight. Blend films were cast on glass slides under three different conditions: (1) at low temperatures (−70 to +20 °C), (2) at ambient temperature (23–25 °C), and at elevated temperatures (47–50 °C). The cast films were approximately 10 μm thick. Film specimens were dried at 70 °C in a vacuum oven at least 24 h and stored in a desiccator prior to experiments.

B. Methods. A Leitz optical microscope (Model Laborlux 12 Pol) was employed in obtaining optical micrographs of the phase-separated domains. Polaroid Instant Camera (Land Film Holder Model 545) was used for small-angle light-scattering (SALS) pictures. For time-resolved light scattering, it is equipped with a two-dimensional Vidicon camera (Model 1252B) controlled by Optical Multichannel Analyser (OMA III, EG&G Princeton Applied Research) coupled with a detector controller (Model 1460). Post data treatments such as background subtraction, sensitivity correction, signal smoothing, and averaging were performed with an off-line computer (IBM PC-XT). A 2-mW He–Ne laser (Spectra Physics Model 102) having a wavelength of 6328 Å was used as a monochromatic light source. A collimated hot stage with an aperture of 2-mm diameter was utilized as a sample cell. Differential scanning calorimetric (DSC) thermograms of the blends were acquired with a Du Pont 9900 DSC apparatus. Most scans were acquired at 20 °C/min unless indicated otherwise.

III. Results and Discussion

A. Effect of Solvent Casting Temperature. Blend films of PC/PMMA cast from THF solutions at low temperatures (below 20 °C) were all cloudy. Optical microscopic studies of these films showed large phase separated regions, familiar to immiscible polymer pairs. Tiny birefringent entities were present within these domains when viewed under cross polarization. However, the blends cast at ambient temperature of 23 °C exhibited translucent appearance. Figure 1 shows a typical optical micrograph of the PC/PMMA (30/70) composition in which small droplets are dispersed. These droplets appear to be birefringent under polarized microscope but are very faint.

This scenerio is best explained in terms of the light scattering images shown in Figure 2. H_v (horizontal polarizer with vertical analyser) scattering reveals a four-lobe clover pattern and an inner diffused halo.[14] The corresponding V_v (vertical polarizer with vertical analyzer) scattering reveals only an intense scattering halo. According to the light scattering theory of Stein–Wilson,[15] the four-lobe image can be associated with orientation fluctuations arising from spherulitic superstructure. The diffused scattering halo occurs as a result of Fraunhofer diffraction of phase-separated domains and is associated with concentration fluctuations. Due to the properties of Fourier inversion, the smaller scattering halo implies the larger periodicity of the phase-separated domains relative to the size of spherulitic structure. In other words, phase-separated domains outgrow spherulites such that crystallization occurs within such domains.

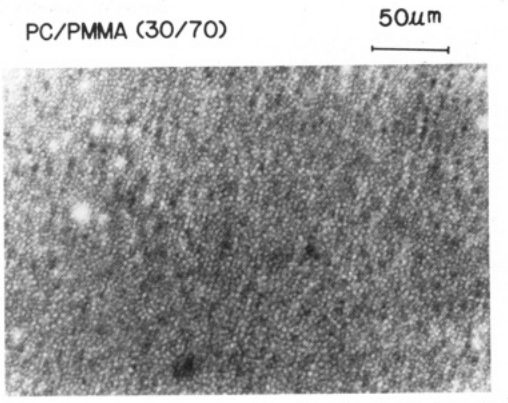

Figure 1. An optical micrograph of PC/PMMA (30/70) composition cast from THF solutions at ambient (23 °C).

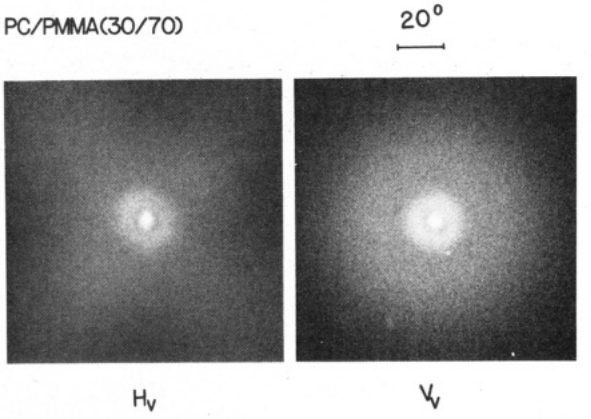

Figure 2. H_v and V_v scattering patterns of various PC/PMMA (30/70) composition cast from THF solutions at ambient (23 °C).

A contrasting observation was made by Hashimoto and co-workers[13] in the blends of polypropylene (PP) with ethylene–propylene rubber (EPR). H_v light-scattering images in their case consisted of a four-lobe clover surrounded by a diffused-scattering halo. The corresponding V_v scattering also showed a two-point pattern encircled by a large scattering ring. They concluded that the crystallization of PP phase exceeded the phase separation process, that is phase separation occurred within the PP spherulitic domains.

Figure 3 represents an intermediate case where the H_v scattering reveals four-lobe images superimposed by more intense scattering arcs contributing at smaller angles. The pure PC exhibits a typical four-lobe pattern characteristic of spherulitic textures. The size of the four-lobe image remains unchanged with the addition of PMMA, but the inner arcs tend to intensify. The diameter of the inner arcs appearing at odd multiples of 45° azimuth is found comparable with that of the V_v scattering ring, suggesting that both scatterings arise from the same origin. It seems that

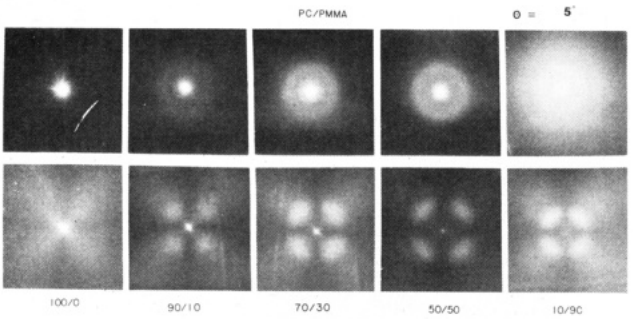

Figure 3. V_v and H_v scattering patterns of various PC/PMMA blends cast from THF solutions.

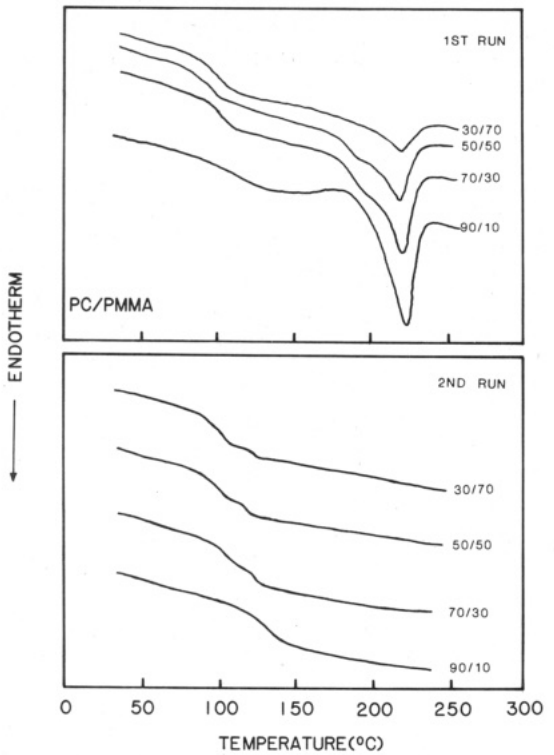

Figure 4. DSC traces of various PC/PMMA blends cast from THF solutions at 23 °C at a high heating rate of 20 °C/min.

both solvent-induced crystallization of PC and phase separation between PC and PMMA occur at comparable rates. PC spherulites appear to fill in PC-rich domains such that the phase-separated domains appear birefringent, thus contributing to scattering at odd multiples of 45° azimuth. It becomes apparent that the final blend morphology is largely controlled by the competition between the solvent-induced crystallization and phase separation processes.

The presence of PC crystals in the PC/PMMA blends can further be confirmed in the following DSC studies. Figure 4 shows the crystal melting temperature (T_m) which remains fairly constant with blend composition. Due to the pronounced crystal melting endotherm, the glass transition temperature (T_g) of pure PC is not as prominent as in pure amorphous PC. However, the intermediate compositions show dual weak T_gs corresponding to those of pure components. In the second runs after quenching from the melt state (300 °C), no crystal melting endotherms are present; however, the two T_gs become more distinct in most compositions. The DSC results support the idea obtained previously from light-scattering studies that solvent-induced phase separation has taken place during solvent (THF) evaporation and is also accompanied by the crystallization of PC phase.

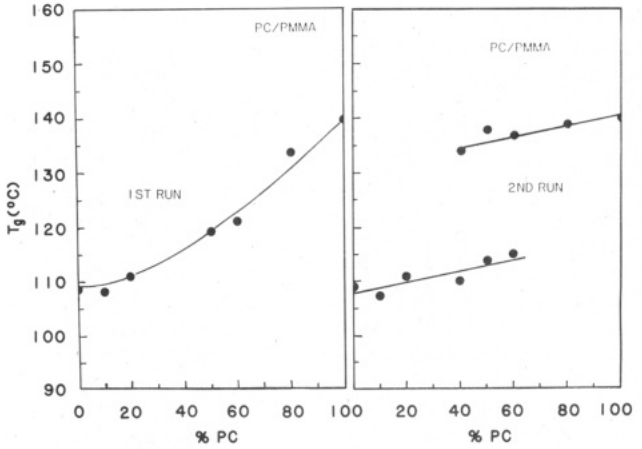

Figure 5. Change of T_g as a function of composition for PC/PMMA blends cast from THF solutions at elevated temperature of 47 °C.

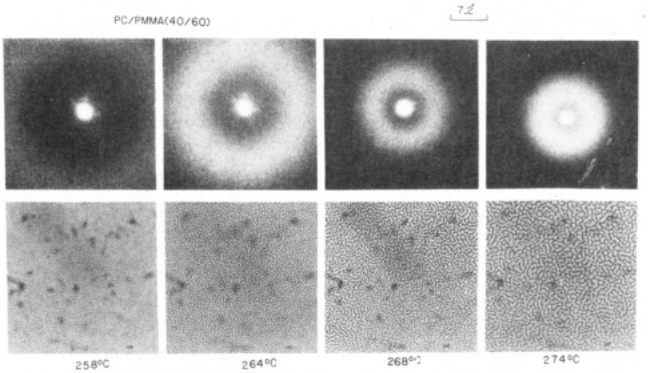

Figure 6. Development of SALS halo and interconnected domains of PC/PMMA (40/60) blends during heating. The optical micrographs were magnified 160 times.

When the PC/PMMA blend films were cast from THF solutions at elevated temperatures (typically 47 °C), the films were completely transparent and scattered no light, characteristic of miscible polymer blends. Figure 5 illustrates a variation of the T_gs of the transparent blend films with blend compositions. Only a single glass transition was observed in all blends, varying systematically with composition, suggestive of polymer miscibility between PC and PMMA. No crystal melting endotherms were discernible in pure polymers as well as in their blends. In the subsequent runs, after heating up to 300 °C, the intermediate blends exhibited clear dual T_gs, implying that thermal-induced phase separation may occur during the course of heating.

To confirm the thermal-induced phase separation, the evolution of phase structure of the PC/PMMA (40/60) blend has been pursued as a function of temperature by using optical microscope and light scattering. Figure 6 shows such micrographs obtained at a heating rate of 10 °C per minute without requiring any polarizers. Phase-separated domains develop at 258 °C and are interconnected. These domains grow with continued heating. The corresponding scattering halo appears large initially, but it collapses to a smaller size with increasing temperature. The revelation of high level of interconnectivity and the clear scattering halo strongly suggest that the thermal-induced phase separation occurs probably through spinodal decomposition and its subsequent coalescence mechanism. When phase-separated domains are observed optically, it is obvious that the phase separation process must be so well advanced that it is already in the late stage of spinodal decomposition. Phase separation, therefore, must be oc-

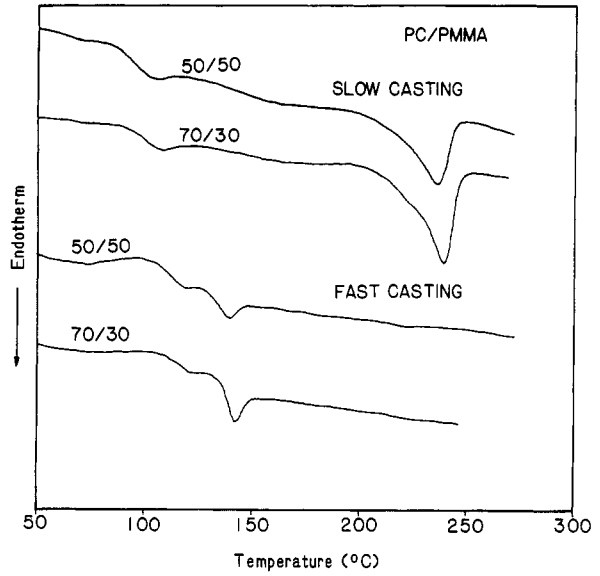

Figure 7. A comparison of DSC traces for PC/PMMA blends cast from THF solutions with and without a cover glass.

curring at relatively low temperatures. This aspect will be reported in a subsequent paper in considerable detail.[16]

B. Effect of Solvent Casting Rate. In the case of PC/PMMA/THF system, the rate of solvent evaporation seems as important as the casting temperature. When blend films were cast in open air in the fume hood, the casting process was completed within 10 min while the casting with a cover took about an hour. Figure 7 shows a comparison of DSC traces for the two different casting conditions all scans invariably reveal dual T_gs. Crystal melting endotherms are not discernible in the former case but are clearly seen in the latter case. T_m does not vary with composition, because the system has already phase separated. When solvent casting is very fast, the solvent-induced crystallization has been prohibited due to lack of adequate time, but it is still long enough for phase separation to occur. This, in turn, suggests that phase separation must be occurring at a faster rate than does crystallization.

The effect of casting rate on phase separation and crystallization is further identified with PC/PMMA/MC and PC/PMMA/CHN systems. Figures 8 and 9 show the DSC results of various blends of PC/PMMA films cast from MC and CHN solutions. Solvent casting is the fastest for MC solution while the casting from CHN is the slowest among the three solvents used. The films prepared from MC solutions show no crystal melting endotherms corresponding to that of PC. Lack of crystallinity in PC was also reported by Varnell et al.[10] in the PC/PCL/MC system. However, two distinct T_gs are observed in the intermediate compositions in both the first and second runs, suggesting that the system results in phase separation during solvent casting. Optical microscopic investigations on these films reveal highly interconnected domains characteristic of spinodal decompositions. V_v scattering shows a halo ring, but there is no scattering with H_v configuration which confirms the previous results that crystallization is not involved in the PC/PMMA/MC system.

In the case of PC/PMMA/CHN system, a prominent crystal melting endotherm can be seen in the pure PC as well as its blends with PMMA. Dual T_gs are also discernible but not pronounced. In the subsequent runs, the PC crystals melt away and do not recrystallize during cooling. The T_gs are well-separated and distinct. Since the evaporation of CHN solution is considerably slow, casting in the fume hood under airflow or with a cover invariably gives the same results, indicating the occurrence of phase separation and crystallization during solvent evaporation. Casting from CHN solution at elevated temperatures of 70 and 100 °C followed the same pattern. There is no appreciable difference between the two grades of PMMA used. The optical micrographs and light scattering patterns of PC/PMMA blends cast from CHN solutions are similar to those obtained from PC/PMMA/THF systems.

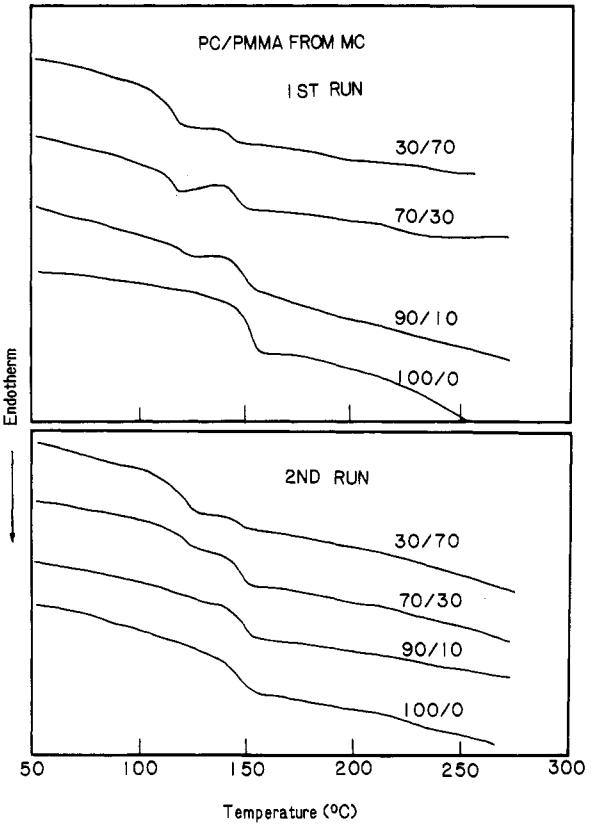

Figure 8. DSC scans of various PC/PMMA blends cast from MC solutions.

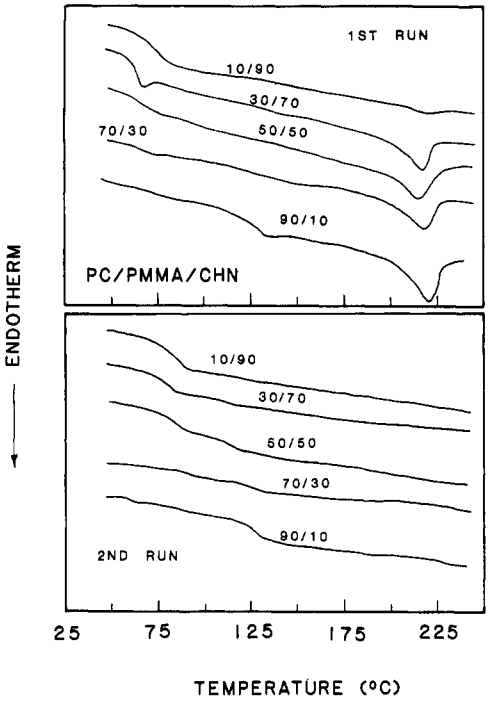

Figure 9. DSC scans of various PC/PMMA blends cast from CHN solutions.

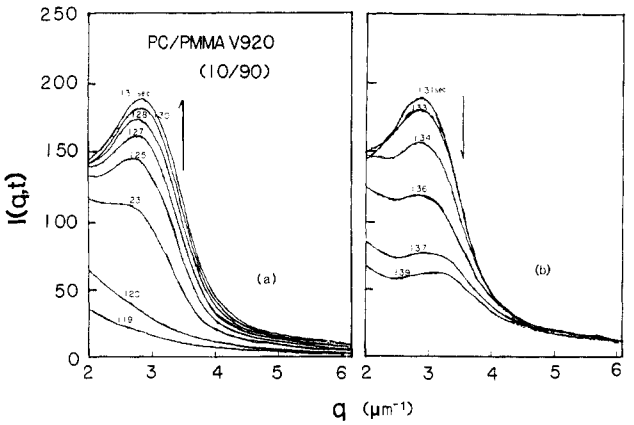

Figure 10. Time evolution of scattering curves of PC/PMMA (10/90) during solvent casting from THF solutions.

The drastic variation of blend morphology depends not only on the casting temperature and the rate of solvent evaporation but also on the type of solvents used. The influence of the solvent type on the phase evolution may be associated with the differences in vapor pressure and hence evaporation rate. Moreover, it also depends upon the specific interaction of the solvent with the respective polymers. It seems that the system mobility at and after the onset of phase separation and/or crystallization is crucial to the evolution of the blend morphology. This has led to time-resolved light-scattering studies on the crystallization and spinodal decomposition of PC/PMMA/THF and PC/PMMA/MC systems.

C. Time-Resolved Light-Scattering Studies of PC/PMMA/THF Systems. Time evolution of scattering profiles of PC/PMMA/THF solutions during solvent evaporation was quantitatively measured by using time-resolved light-scattering setup described in a previous paper.[17] A typical set of light-scattering curves for the PC/PMMA (10/90) composition obtained under V_v configuration is depicted in Figure 10. The peak intensity increases in the early phase of solvent evaporation then decreases and comes to a standstill as the polymer concentration approaches the dry state. The peak position remains stationary throughout the casting process. This suggests that the phase-separated domains are not getting larger but merely that the gradient of concentration fluctuations is increasing. This kind of behavior has already been predicted by Cahn's linearized theory of spinodal decomposition for incompressible binary mixtures.[18]. Strictly speaking, the extension of Cahn's theory[18] originally developed for binary systems to our ternary system containing solvent as one component is questionable. However, THF is a good solvent for both PC and PMMA, and one may approximate PC/PMMA/THF as a pseudobinary system by taking into consideration the PC/THF as one phase and PMMA/THF as the other. In this context of the pseudobinary approximation, the analyses will be undertaken.

In the early stage of spinodal decomposition, the growth of spatial concentration fluctuations of a binary mixture may be expressed as

$$\Delta C(\mathbf{r}) = \sum \exp[R(q)t]\{A(q) \cos(\mathbf{q}/\mathbf{r}) + B(q) \sin(\mathbf{q}/\mathbf{r})\} \quad (1)$$

where $\mathbf{r}$ is the position vector and $q = 4\pi/\lambda \sin(\theta/2)$. λ is the wavelength of light, and θ is the scattering angle measured in the medium. $R(q)$ is the amplification factor characterizing the growth rate of the fluctuations which is further given by

$$R(q) = -Mq^2\{(\partial^2 f/\partial c^2) + 2\kappa q^2\} \quad (2)$$

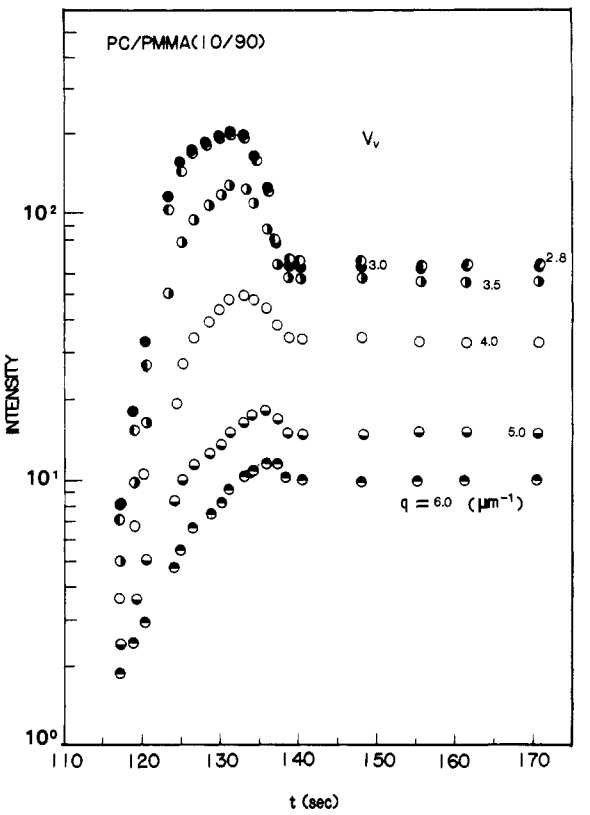

Figure 11. Log I versus t plots for various wavenumber (q) for PC/PMMA (10/90).

where f is the free energy, c represents the concentration, κ is the composition gradient coefficient, and M is the mobility. Equations 1 and 2 were obtained without considering the nonlinear high-order terms in the modified diffusion equation. The linearized Cahn's theory predicts that time dependence of scattered light (X-rays or neutrons) has the form

$$I(q,t) = I(q,t = 0) \exp\{2R(q)/t\} \quad (3)$$

where t is the phase separation time.

According to eq 3, the plot of log I versus t should give a straight line at least in the early period of phase separation from which $R(q)$ can be determined. Figure 11 represents such a plot for the PC/PMMA (10/90) composition cast from 2% THF solutions. The intensity appears to increase exponentially in early period as predicted by the linearized theory, then exhibits a maximum, and decreases to limiting intensity values for various wavenumbers (q). The initial increase of the scattered intensity is approximated by a slope from which $R(q)$ may be determined from a given q. Subsequently, $R(q)/q^2$ is plotted against q^2 in Figure 12 in order to determine the diffusivity $D = M(\partial^2 f/\partial c^2)$ from the intercept and the coefficient of concentration gradient κ from the slope. As can be seen in Figure 12, the curves are not necessarily linear; some deviations are particularly seen at small q regions. This kind of deviation is commonly observed in thermal-induced phase separation of many binary polymeric mixtures.[5,7,8] Hashimoto and co-workers treated their ternary PB/PS/Tol and SB/PS/Tol systems as pseudobinary system but found that the linearized Cahn's theory to be operative.

In the present case, the scenerio is more complex as PC phase can undergo crystallization especially when cast from THF solution. It is well-known that V_v scattering is contributed by many factors such as concentration or density fluctuations, orientation fluctuation, optical anisotropy, and refractive index of surrounding medium while H_v

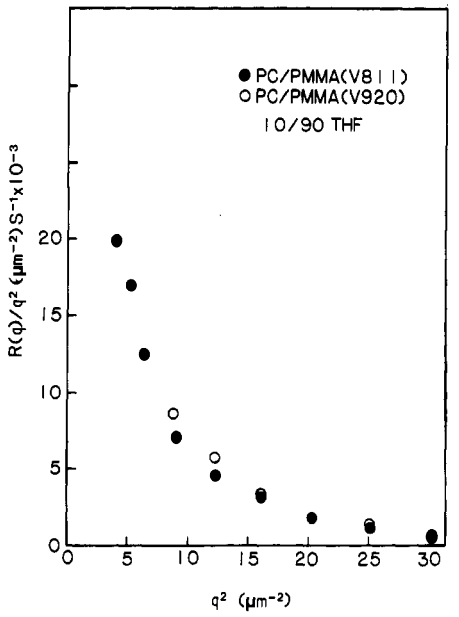

Figure 12. $R(q)/q^2$ versus q^2 plots of various PC/PMMA (10/90) blends.

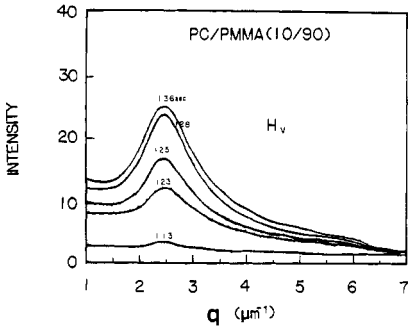

Figure 13. Time evolution of H_v scattering curves of PC/PMMA (10/90) during solvent casting from THF solutions.

scattering exclusively arises from orientation fluctuations. Hence, the crystallization of PC phase can be directly followed by monitoring H_v scattering. Figure 13 shows the time evolution of H_v scattering if the PC/PMMA (10/90) during solvent casting from THF under equivalent conditions. A maximum corresponding to the inner lobe of Figure 2 develops around 120 s and increases initially with time then levels off as solvent continues to dry out. The peak position, however, remains stationary throughout the phase separation process. As has been pointed out previously, solvent-induced crystallization of PC occurs within the phase-separated domains. Hence, the time evolution of H_v maximum represents the crystallization process.

Figure 14 shows the comparison of time dependence of the V_v and H_v scattered intensity of the PC/PMMA (10/90) blends during casting from THF solutions. The V_v scattering appears to increase exponentially in the early stage and shows a maximum before it levels off. The H_v scattering, on the other hand, occurs considerably slower than that of the V_v scattering, without showing any intensity shootup. The time at which the H_v scattering arises roughly corresponds to that where the V_v intensity is maximum, which implies that the intensity overshoot in V_v configuration may be associated with the crystallization of PC. Such intensity variation of V_v scattering can be readily explained on the basis of the classical theory of Stein and Rhodes.[19]

The light scattering theory[19] predicted that as crystallization proceeds, V_v scattering will increase first until it reaches a maximum, then decreases, and increases again subsequently. The V_v image is initially isotropic, becomes more intense, and then changes to anisotropic pattern. This scenerio has been explained on the basis of changing refractive indices of the surrounding medium that controls the relative contributions arising from concentration fluctuations and orientation fluctuations. In the present case, phase separation has been progressing while crystallization takes place during solvent evaporation which will undoubtedly cause changes in the refractive indices of the surrounding medium. The final V_v pattern is circular which suggests that the scattering must be dominated by the contribution of concentration fluctuations of the phase separated domains. It should be emphasized that phase separation occurs first and then is accompanied by crystallization of PC phase.

IV. Time-Resolved Light-Scattering Studies of PC/PMMA/MC Systems

The solvent casting of the 10/90 (PC/PMMA) blend from MC solutions behaves rather differently from that observed for PC/PMMA/THF systems. As mentioned

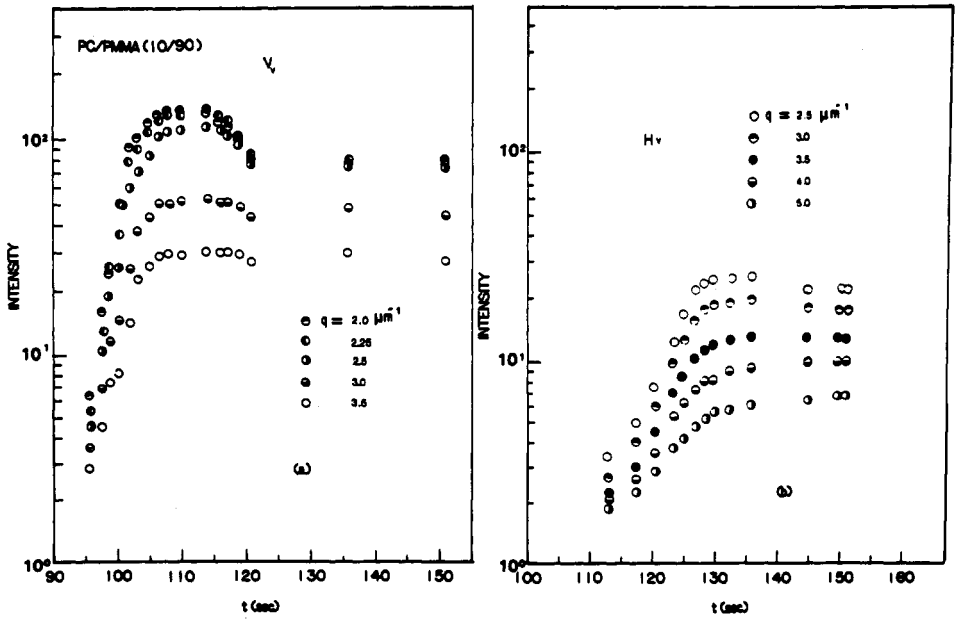

Figure 14. A comparison of log I versus t curves of PC/PMMA (10/90) under V_v and H_v SALS configurations.

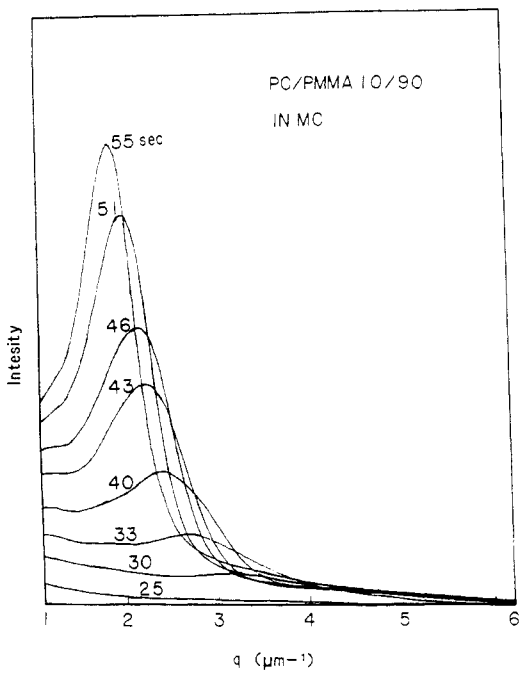

Figure 15. Time evolution of V_v scattering curves of PC/PMMA (10/90) during solvent evaporation from MC solutions.

before, PC phase does not undergo crystallization when cast from MC solution, thus there is no H_v scattering. Time evolution of V_v scattering cures are displayed in Figure 15 in which the first scattering appears appreciably faster than that of the PC/PMMA/THF system. There is no noticeable period during which the peak remains at a constant position; thus the linearized Cahn's theory seems invalid here. The peak shifts to lower scattering angles while it continues to intensify. This contrasting behavior may be associated with the very fast evaporation rate of MC such that the initial period is not detected. By the time the solvent-induced phase separation is observed optically, the process may be so well advanced that we are practically observing the late stage of spinodal decomposition.

The late stage of spinodal decomposition in binary mixtures was studied by Binder and Stauffer,[20] who considered that clusters aggregate by a diffusion process and coalesce into larger clusters associated with a decrease in free energy of the system. The reiteration of this process causes an increase in the cluster size $R(t)$ in a simple form of the power law

$$R(t) \propto t^{\alpha} \tag{4}$$

or in an equivalent expression

$$q_{max}(t) \propto t^{-\alpha} \tag{5}$$

and

$$I_{max}(t) \propto t^{\beta} \tag{6}$$

with the relationship $\beta/\alpha = 3$. Siggia[21] predicted that the late stage of spinodal decomposition occurs through coarsening mechanism driven by the surface tension in which case $\alpha = 1$.

Figure 16 and 17 exhibit the logarithmic plots of q_{max} and I_{max} as a function of phase separation time t. The plot of log q_{max} versus log t can be represented by a slope of -1 while the plot of log I_{max} versus t gives a slope of 3. Hence, this regime is characterized by the late stage of spinodal decomposition where the power law scheme prevails. The value $\alpha = 1$ is exactly the value predicted by Siggia for binary liquids.

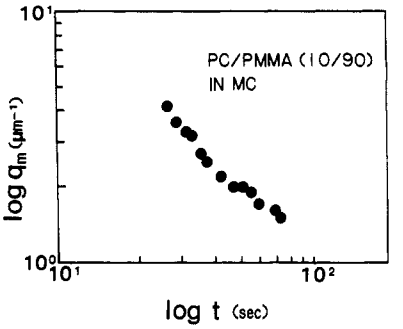

Figure 16. Logarithmic plot of q_{max} versus t for PC/PMMA (10/90) during solvent evaporation from MC solutions.

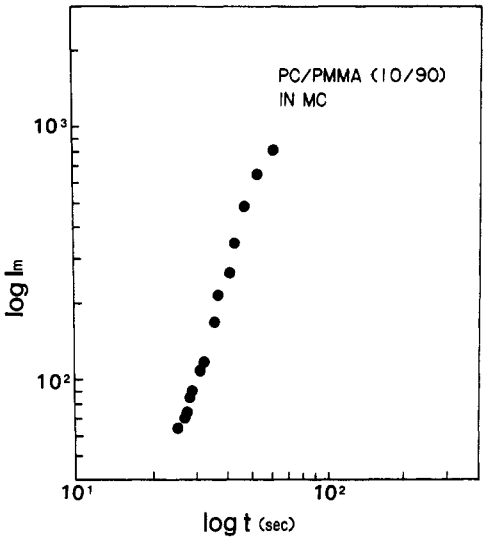

Figure 17. Logarithmic plot of I_{max} versus t for PC/PMMA (10/90) during solvent evaporation for MC solutions.

Although these data fit reasonably well with the model proposed by Siggia for the late stage of phase separation within the spinodal region, the early stage is not observed in the MC case. In fact, the MC evaporates much more rapidly during the solvent casting process than does THF. Thus the percentage of solvent present is probably also undergoing considerable change during the phase separation process. This will expedite the SD process; hence, there is a possibility that the early stage may be totally undetected. Also, because of the rapid evaporation of the MC, the PC has no time to crystallize. This observation may be in contrast with the CHN case, where the solvent evaporation is very slow so that crystallization of PC can take place. The behavior of phase separation in the CHN case is quite similar to that of the THF; thus the time-resolved data is not elaborated further. Since the present polymer/polymer/solvent system is extremely complex, it should be of interest to test the existing theories with thermally induced phase separation of this PC/PMMA binary system. The study will be reported in a subsequent paper.[16]

V. Conclusions

We have demonstrated the profound sensitivity of solvent casting on the final morphology of PC/PMMA blends. When blend films were cast from THF solutions, it seems possible to obtain a completely miscible or immiscible or partially miscible blend by carefully controlling the environmental temperature. In the totally immiscible case, crystallization of PC takes place within the phase-separated domains. If the rate of solvent casting from THF is sufficiently fast, crystallization does not occur. The casting from CHN solutions invariably results in phase

separation accompanied by crystallization of PC phase. The casting from MC solutions gives modulated structure, but no crystallization is involved. Time-resolved light scattering studies on PC/PMMA/THF system is characterized by the early stage of spinodal decomposition; however, the linearized Cahn's theory is found inadequate. In the case of PC/PMMA/MC system, the power-law scheme prevails characterizing the late stage of spinodal decomposition.

Acknowledgment. A partial support from Edison Polymer Innovation Corp. (EPIC) is gratefully acknowledged.

Registry No. PC (copolymer), 25037-45-0; PC (SRU), 24936-68-3; PMMA, 9011-14-7.

References and Notes

(1) Olabisi, O.; Robeson, L. M.; Shaw, M. T. *Polymer Polymer Miscibility*; Academic: New York, 1979.
(2) MacMaster, L. P. *Adv. Chem. Ser.* **1975**, *No. 142*, 43.
(3) Nishi, T.; Wang, T. T.; Kwei, T. K. *Macromolecules* **1975**, *8*, 227.
(4) Gilmer, J., Goldstein, N., and Stein, R. S., *J. Polym. Sci., Polym. Phys. Ed.* **1982**, *20*, 2219.
(5) Nojima, S.; Nose, T. *Polym. J.* **1982**, *14*, 269; **1982**, *14*, 907.
(6) Hashimoto, T.; Kumaki, J.; Kawai, H. *Macromolecules* **1983**, *16*, 641.
(7) Snyder, H. L.; Meakin, P.; Reich, S. *Macromolecules* **1983**, *16*, 757.
(8) Hill, R. G.; Tomlins, P. E.; Higgins, J. S. *Macromolecules* **1985**, *18*, 2555.
(9) Voigt-Martin, I. G.; Leister, K. H.; Rosenau, R.; Koningsveld, R. *J. Polym. Sci., Polym. Phys. Ed.* **1986**, *24*, 723.
(10) Varnell, D. F.; Runt, J. P.; Coleman, M. M. *Macromolecules* **1981**, *14*, 1350.
(11) Inoue, T.; Ougizawa, T.; Yasuda, O.; Miyasaka, K. *Macromolecules* **1985**, *18*, 57.
(12) Zeeman, K.; Patterson, D. *Macromolecules* **1972**, *5*, 513.
(13) Hashimoto, T.; Sasaki, K.; Kawai, H. *Macromolecules* **1984**, *17*, 2812. Sasaki, K.; Hashimoto, T. *Macromolecules* **1984**, *17*, 2818.
(14) Note that H_v cross polars are slightly offset in order to accentuate the inner scattering halo.
(15) Stein, R. S.; Wilson, P. R. *J. Appl. Phys.* **1962**, *33*, 1914.
(16) Kyu, T.; Saldanha, J. M., *Macromolecules*, submitted for publication.
(17) Kyu, T.; Saldanha, J. M. *J. Polym. Sci., Polym. Lett. Ed.*, submitted for publication.
(18) Cahn, J. W. *J. Chem. Phys.* **1965**, *42*, 93.
(19) Stein, R. S.; Rhodes, M. B. *J. Appl. Phys.* **1960**, *31*, 1873.
(20) Binder, K.; Stauffer, D. *Phys. Rev. Lett.* **1974**, *33*, 1006.
(21) Siggia, E. D. *Phys. Rev. A* **1979**, *20*, 595.

Configurational Properties of a Terminally Attached Chain at the Boundary of a Molecularly Coarse Solvent

Clive A. Croxton

Department of Mathematics, University of Newcastle, NSW 2308, Australia.
Received January 20, 1987

ABSTRACT: The effect of solvent composition (solvent particle diameter and packing fraction) upon the configurational properties of hard-sphere chains terminally attached to a rigid boundary is investigated on the basis of the iterative convolution (IC) approximation. It is found that the segment density profile normal to the boundary develops pronounced oscillations of period equal to the solvent diameter and amplitude depending upon solvent packing fraction. The contact amplitude at the boundary develops dramatically as solvent diameter decreases, with important implications for the development of loop and train configurations. We also find that the mean thickness of the adsorbed layers, the mean square end-to-end length, and the mean square radius of gyration all decrease with the introduction of solvent.

Introduction

Considerable theoretical attention has been focused on the description of the configurational properties of terminally attached chains in the vicinity of a rigid plane boundary since the problem has implications for a wide variety of phenomena ranging from applications in chemical engineering to aspects of cell biology. These studies may be broadly resolved into lattice-based and continuum analyses in which a variety of exact enumeration, Monte Carlo, and other analytical and numerical techniques have been applied. While the self-avoiding feature is accounted for to a varying and approximate degree in these studies, the role of the solvent in determining the configurational properties of the chain has received little attention. Certainly, chains embedded in a regular lattice to a certain degree reflect the molecular coarseness of the solvent, but only in as far as the lattice provides an adequate representation of the surrounding fluid, which by any other standard it does not. Nevertheless, in an earlier study by Bellermans and De Vos,[1] the ratio of the mean-square lengths $\langle R_{1N}^2\rangle_\eta/\langle R_{1N}^2\rangle_{\eta=0}$ for athermal chains embedded in a simple cubic lattice was investigated as a function of chain packing fraction η. Each site may be occupied either by one element of a chain molecule or by a solvent molecule. At low to intermediate concentrations the ratio decreases almost linearly with η:

$$\langle R_{1N}^2\rangle_\eta/\langle R_{1N}^2\rangle_{\eta=0} \sim 1 - 0.04(N-1)^{0.7}\eta + \ldots$$

A similar, but nonlinear, dependence was found on the basis of a continuum convolution analysis at intermediate to high packing fractions,[2] becoming quadratic ($N < 11$) and then cubic ($12 < N < 20$) with increasing chain length.

In a previous publication[2] we reported the configurational properties of an isolated athermal self-avoiding chain in a solvent of its own segments on the basis of a convolution integral approximation. The results were extended to include the equation of state at intermediate to high polymer packing fractions, and recent Monte Carlo simulations appear to be in excellent agreement with those predictions.[3] Since then, the technique has been superseded by an iterative convolution approach (IC), which for short to intermediate length sequences ($N < 25$ segments) appears to yield configurational properties in good quantitative agreement with Monte Carlo simulation studies.[7]

It was found that the spatial probability distributions $Z(r_{ij}|N)$ of segments i,j within the isolated N-mer were

0024-9297/87/2220-2847$01.50/0